

Clinical applications of deep learning in distinguishing Benign from Malignant Pulmonary Nodules in CT Scans

Keywords

malignant tumor, pathology, morphological detection, radiology, oncology

Abstract

Background: Early diagnosis is crucial for improving lung cancer prognosis, a leading cause of cancer-related deaths. Lung cancer includes small cell lung cancer (SCLC, ~15% of cases) and non-small cell lung cancer (NSCLC, ~80–85%). Prognosis depends on the stage at diagnosis; the 5-year survival rate is 65% for localized NSCLC but only 9% for distant-stage disease. Radiologists face challenges distinguishing benign from malignant pulmonary nodules on CT scans.

Aims/Methods: This review explores deep learning (DL) methods, including multi-view Convolutional Neural Networks (CNNs) and 3D models for nodule segmentation, emphasizing volumetric assessments for malignancy prediction.

Results: CNNs effectively analyze CT data, achieving 94.2% sensitivity with 1.0 false positives per scan in lung nodule detection.

Conclusion: DL enhances diagnostic accuracy, reduces radiologist workload, and enables earlier lung cancer detection. Further research is needed to improve model adaptability across diverse clinical settings.

Preprint

1
2
3
4
5
6
7
8
9
10
11
12
13
14
15
16
17

**Clinical applications of deep learning in distinguishing Benign from Malignant Pulmonary
Nodules in CT Scans**

Yongzhong Xu^{1,#}, Yunxin Li¹, Feng Wang¹, Yafei Zhang¹, Delong Huang¹
1-Imaging Department, Yantaishan Hospital, Yantai, Shandong 264003, China

#Corresponding author: Yongzhong Xu, email is 13220931662@163.com.

Preprint

18

19 **Abstract:**

20 **Background:** Early diagnosis is crucial for improving lung cancer prognosis, a leading cause of
21 cancer-related deaths. Lung cancer includes small cell lung cancer (SCLC, ~15% of cases) and
22 non-small cell lung cancer (NSCLC, ~80–85%). Prognosis depends on the stage at diagnosis; the
23 5-year survival rate is 65% for localized NSCLC but only 9% for distant-stage disease.

24 Radiologists face challenges distinguishing benign from malignant pulmonary nodules on CT
25 scans.

26 **Aims/Methods:** This review explores deep learning (DL) methods, including multi-view
27 Convolutional Neural Networks (CNNs) and 3D models for nodule segmentation, emphasizing
28 volumetric assessments for malignancy prediction.

29 **Results:** CNNs effectively analyze CT data, achieving 94.2% sensitivity with 1.0 false positives
30 per scan in lung nodule detection.

31 **Conclusion:** DL enhances diagnostic accuracy, reduces radiologist workload, and enables earlier
32 lung cancer detection. Further research is needed to improve model adaptability across diverse
33 clinical settings.

34 **Keywords:** malignant tumor/pathology/morphological detection /radiology and oncology

35

36

37 Introduction

38 Lung cancer is one of the most deadly malignancies that can endanger a person's life or health[1].
39 Many nations have seen lung cancer incidence and death rise during the last 50 years [2]. The
40 American Cancer Society (ACS) projected 608,570 fatalities and 1,898,160 new cases in 2021 [3].
41 As a prominent radiological signal, lung nodules are used to diagnose lung cancer early. Diameter
42 determines nodule malignancy[4]. Nodules in the pulmonary interstitium, which consists of the
43 basement membrane, pulmonary capillary endothelium, alveolar epithelium, and perilymphatic
44 and perivascular tissues, are typically small, spherical, and circumscribed [5, 6]. Lung nodules
45 vary in size, shape, and kind[7]. Nodules can vary in size from less than 2 mm to 30 mm, and some
46 of them are hard to spot because of their complex circulatory connections in places with plenty of
47 vessels [8]. There are certain solid and sub-solid nodules (SSNs) with densities that are marginally
48 greater than those of the parenchyma of the lung [9]. SNs are the most common nodules and
49 comprise the core functioning lung tissues, while SSNs are lung cancer with minimal transparency
50 in the ground glass. SSNs may be part-solid or pure ground glass [10]. These nodules do not block
51 bronchovascular networks, but their opacifications are denser than those of the surrounding tissues
52 [7].

53 Accurate nodule diameter measurements are essential for diagnosis since nodule size is correlated
54 with malignancy. Several studies [5, 11, 12] offer valuable insights[13]. The End-Use Load and
55 Consumer Assessment Program (ELCAP) database [3] reports a 1% malignancy risk for nodules
56 under 5 mm, 24% for 6–10 mm, 33% for 11–20 mm, and 80% for 20+ mm [14]. However,
57 measuring the diameters of extremely small nodules may result in errors. The therapy for cancer
58 of the lung nodules is complicated. Almost 70% of individuals with lung cancer require radiation
59 treatment, however radiation-induced lung damage may reduce treatment rates and raise morbidity

60 and death. Radiologists need computer-aided diagnostic (CAD) technologies to extract more
61 information from nodules and enhance classification accuracy. CAD systems minimize
62 observational errors, false-negative rates, and medical image interpretation and diagnostic second
63 opinions [15, 16]. Numerous studies indicate that CAD systems improve image diagnosis and
64 lower inter-observer variance. [17]. CAD systems can also quantify clinical decisions like biopsy
65 recommendations [18], help diagnostic checks, minimize thoracotomies and false-positive
66 biopsies [16, 19], and distinguish tumor malignancies [20, 21]. Clinical success has led to the
67 introduction of CAD models for lung cancer diagnosis. Early diagnosis of lung nodules may
68 improve survival using such devices. Current CT (Computed tomography) CAD applications
69 search for spherically distributed lung nodule-like pulmonary densities [15]. Thus, lung nodule
70 screening by CT CAD is a hot topic. Lung nodule detection initially was based on non-machine
71 learning techniques [22-28]. Later, data-driven machine learning-based algorithms [29-34] built
72 the ideal border [35]. Deep learning (DL) inspired algorithms have recently attracted interest
73 because of their precise predictions. Unlike traditional CAD systems, DL-based models might be
74 optimized and applied to vast volumes of data [36]. DL using CNNs has improved pulmonary
75 nodule diagnosis and treatment [37-40]. Three modules of DL are used to recognize, segment, and
76 categorize lung nodules. Detection identifies the nodule, segmentation delineates its voxels, and
77 classification determines whether it is benign or malignant [35].

78 Lung cancer often remains asymptomatic in its early stages, leading to delayed diagnoses. When
79 symptoms appear, they frequently include shortness of breath, wheezing, hoarseness, chest pain,
80 coughing up blood, and a persistent cough. Additional signs may involve recurrent respiratory
81 infections, unexplained weight loss, and fatigue. Moreover, these symptoms might differ from
82 person to person and can mimic those of other respiratory disorders [41].

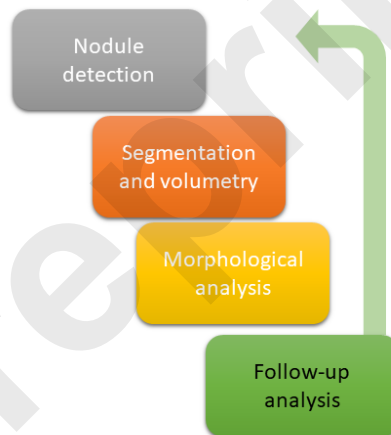
83 Regarding mortality, lung cancer remains a leading cause of cancer-related deaths globally. For
84 instance, in the United States, an estimated 124,730 lung cancer-related deaths are anticipated for
85 2025. The mortality rate is significantly higher in older populations, with three-quarters of lung
86 cancer deaths occurring among those aged 65 and older. Increasing survival rates requires early
87 detection through screening programs since lung cancer can often be identified at an advanced
88 stage when there are few available treatment choices [41].

89 Previous studies have explored the detection approaches for pulmonary nodules [35, 36, 42-48]
90 with various goals. The primary aim of this article is to provide a comprehensive review of deep
91 learning (DL) methodologies employed for pulmonary nodule identification and classification in
92 computed tomography (CT) images. This study aims to explore the effectiveness of various DL
93 models, including multi-view convolutional neural networks (CNNs) and 3D architectures, in
94 improving diagnostic accuracy and efficiency in lung cancer screening. Further, it aims to identify
95 current challenges, such as data variability and the need for external validation, and suggest
96 directions for future research to facilitate the integration of these advanced technologies into
97 routine clinical practice. This study introduces a novel deep learning-based system using two 3D
98 models for automated pulmonary nodule detection, aiming to enhance diagnostic accuracy and
99 reduce false positives.

100 **Detection Nodule**

101 Identifying microscopic pulmonary nodules is challenging yet important for lung cancer diagnosis.
102 Chest volumetric CT images exceed 9 million voxels. Five-mm lung nodules occupy 130 voxels,
103 or 1.4×10^{-5} lung volume [49]. Radiologists may be able to detect these nodules based on their shape,
104 size, density, location, and closeness to adjacent structures. 1.6×10^{18} Early CT screening missed 8.9%

105 of malignancies in the NLST CT screening arm [50]. The pathological analysis of biopsy samples
106 is still the most reliable method for identifying and defining pulmonary nodules, even though
107 imaging approaches are significant for their detection. Although reading a scan simultaneously by
108 two observers improves diagnostic sensitivity, performing it repeatedly is time-consuming and
109 impracticable [51]. This emphasizes the significance of machine-learning technology to assist
110 radiologists detect nodules, one of the most studied CAD applications that reduce the time needed
111 to interpret scans [52]. Several studies have demonstrated that deep learning may improve nodule
112 detection sensitivity. Figure 1 shows the steps in the lung nodule treatment route using AI.



113
114 **Figure 1:** Steps in the lung nodule treatment route, where AI might have a role.
115 This CAD application has been extensively investigated and has been demonstrated to minimize
116 scan interpretation time [52]. Various studies have reported that deep learning can enhance the
117 sensitivity of nodule identification. [53].

118 **Nodule segmentation**

119 Malignancy is highly predicted by nodule size; in the NELSON trial, those with nodules <100
120 mm³ had the same baseline cancer risk (0.5%) as those without nodules [54]. Traditional nodule
121 size assessment involves manual 2D caliper measurement of the biggest transverse diameter.
122 Current screening studies and national and worldwide guidelines on nodule treatment have
123 recommended evaluating volume rather than diameter because it is less susceptible to intra- and
124 interobserver variability [55] better incorporates the three-dimensional (3D) character of a lung
125 nodule [56], is more susceptible to size change, and detects malignancy sooner than 2D diameter
126 measures [57]. Nodule segmentation is essential for volumetric measurements. Numerous CAD
127 methods for nodule segmentation have been developed since the 1980s [44]. Detecting
128 microscopic pulmonary nodules is challenging yet significant for lung cancer diagnosis. Chest
129 volumetric CT images exceed 9 million voxels. Five-mm lung nodules occupy 130 voxels or 1.4
130 10⁻⁵ lung volume. These nodules may be detectable by radiologists depending on their shape, size,
131 density, location, and proximity to other structures. 16e18 Early CT screening missed 8.9% of
132 malignancies in the NLST CT screening arm [58].

133 Subsolid nodules are more challenging to segment than solid lesions because there is less
134 attenuation difference between the tumor and the surrounding parenchyma. It is also more
135 challenging to distinguish the solid component of these very big nodules from nearby vessels.
136 However, current research indicates that these problems can be addressed [59]. Multiple manual,
137 semi-automatic, and automated volumetric analysis software programs have been reported in
138 recent years. Software tools have different size measurements, however, these packages provide
139 reliable repeat measurements. The variance is larger in irregular and juxta-pleural nodules [60].
140 The British Thoracic Society's pulmonary nodule management guidelines suggest reducing
141 variability in nodule volumetry [61].

142 Research has demonstrated that deep learning can improve nodule segmentation. A single click
143 can volumetrically segment 7,927 NLST nodules using a deep learning model. These parameters
144 were used to evaluate the Brock University Cancer Prediction Model's malignancy prediction
145 accuracy. The AUC for volumetric analysis was 88.17, compared to 85.96 for NLST radiologists'
146 2D measurements, demonstrating a 2.21% enhancement in predictive value. As CNN algorithms
147 implicitly segment nodules, deep learning may eliminate nodule segmentation [38, 62].

148 **The issue of detecting lung nodules in daily clinical practice**

149 Lung cancer is the leading cause of cancer death worldwide [63]. Symptoms typically appear after
150 cancer has spread, thus late diagnosis is usual [64]. To detect malignancies early, the US, China,
151 and Korea have implemented nationwide lung tumor screening programs. High-risk individuals
152 (older smokers) are invited for a low-dose CT lung scan in a screening program [65]. Lung cancer
153 may manifest as a "nodule" or spot. Trials show that low-dose CT screening decreases lung
154 carcinoma mortality [66, 67], but Europe and other nations have been sluggish in embracing it.
155 Therefore, early-stage lung cancer is often identified incidentally through nodules observed in CT
156 scans carried out for unrelated medical reasons [68, 69]. It's challenging to see lung nodules. CT
157 scans are highly varied and not specifically intended to identify lung cancer because of the growing
158 diversity of scanning methods and patients [49]. Nodule detection and treatment will become more
159 crucial because radiologists' workload has increased significantly over the past 15 years, primarily
160 due to the demand for CT imaging [70].

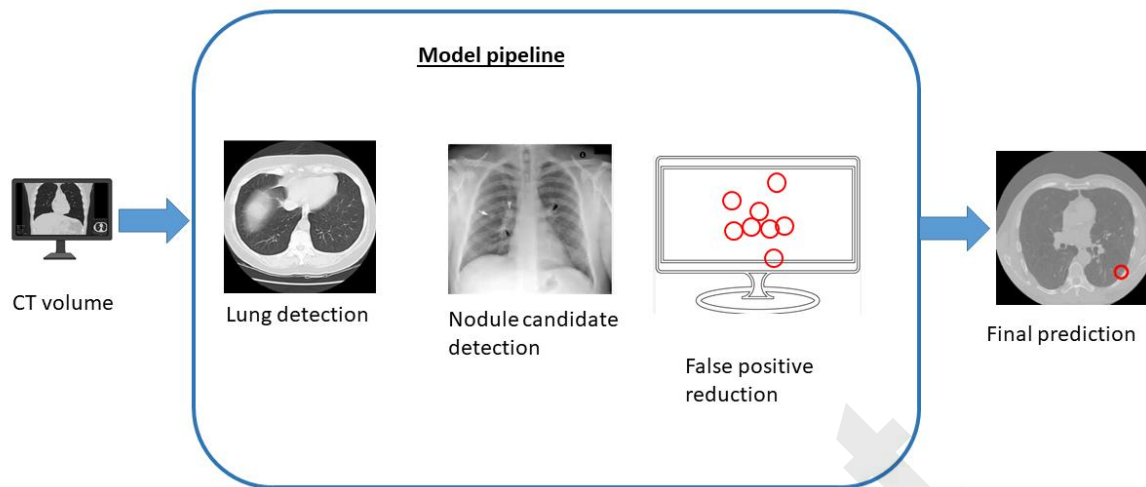
161 **Artificial Intelligence for radiological support**

162 AI software may help radiologists find lung lesions in CT images. The use of AI software as an
163 auxiliary reader enhances radiologists' reading time, management recommendation uniformity,

164 and detection sensitivity [71-74]. A few studies have tried AI solutions in non-screening
165 environments. The generalization performance of the AI software was tested using a multi-center
166 study approach to expand this research area and address three common issues. Second, we used
167 five qualified thoracic radiologists rather than one or two to establish the reference standard
168 because nodule detection varies greatly. Third, and perhaps most importantly, we examined
169 whether an AI system could identify the important nodules using reliable nodule-level malignancy
170 labels. Research on AI has either looked at all nodules (regardless of malignancy) or scan-level
171 cancer detection. Therefore, our effort aims to connect AI investigations for nodule identification
172 and lung malignancy.

173 **Connecting the gap between nodule detection and lung cancer AI studies**

174 The DL-based technique was retrospectively tested for identifying actionable benign nodules
175 (requiring follow-up), minor lung cancers, and metastases in CT images from two Dutch hospitals'
176 typical clinical contexts. Moreover, the nodule detection method locates a specific lung region
177 slice by slice using a CT scan. Five-slice overlapping CT volumes yield nodule candidates. Finally,
178 09 slices from a 3D area around each nodule candidate are inspected for nodules. Nodules from
179 lung arteries and other structures can be promptly identified in CT scans using the 2.5D
180 identification method (Figure 2).

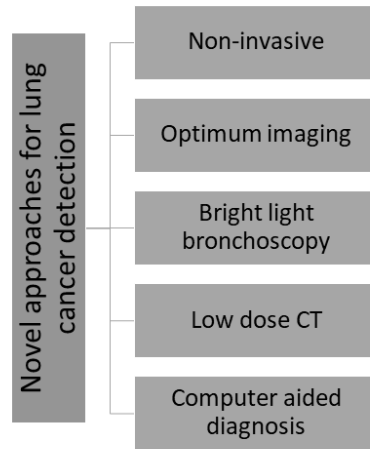


181

182 **Figure 2.** An overview of the planned lung nodule detecting system

183 **DL Strategies for Detecting Lung Cancer**

184 Automation has the potential to assist in diagnosing various diseases through CAD [75]. This
 185 method employs software to identify, predict, and classify symptoms, assisting in identifying the
 186 presence and severity of a disease. This study reviews CAD approaches for lung CT nodule
 187 detection. CT scans can identify nodules of lung cancer, especially large ones in the advanced
 188 stages [76]. The nodules need to be identified early because they are often little before a lung tumor
 189 the size of a golf ball grows. Figure 3 shows that manually distinguishing and segmenting nodules
 190 is challenging.



191

192 **Figure 3.** Methods for lung tumor detection.

193 CNNs are great for image classification. Human visual brain function inspired this architecture.

194 CNN filters assess a small portion of the image by simulating neurons with receptive zones. Deeper
195 layers of these neurons may learn and detect more complicated hierarchical patterns due to their
196 larger receptive fields. CNNs appear to be many sliding windows with small neural networks
197 spread around the image [77].

198 CNNs can learn patterns regardless of location due to their location invariance. The filter can learn
199 image designs using sliding windows. Since CNNs are hierarchical, they can automatically
200 identify more abstract patterns [78]. Boundaries and structures may be occupied by the initial
201 layers, followed by forms in the intermediate layers and overall object shapes in the higher layers.

202 CNNs are capable of analyzing 3D images rather than slices from CT scans. A sliding cube, instead
203 of a movable pane, can be employed to develop 3D CNNs for feature extraction at each stage [79].

204 **Computer-Assisted Lung Cancer Detection Utilizing CT Pictures**

205 CT-based lung tumor identification and detection employing DL algorithms has been the subject
206 of numerous studies. Healthy and unhealthy CT scans have different image attenuation patterns.
207 To separate the lungs from the nearby tissues, numerical, grey-level thresholding, and shape-based
208 methods have been employed [80]. Brown and coworkers introduced an automatic, knowledge-
209 based chest segmentation approach [81]. This approach requires organ volume, relative location,
210 shape, and X-ray attenuation. To extract useful CT image data, Brown et al., developed a
211 knowledge-based automatic segmentation method [82]. They automatically created indirect
212 quantitative values of single lung activities that routine pulmonary function tests cannot. Hu and
213 his coworkers created a completely automated pulmonary segmentation approach from 3-D lung
214 X-ray photographs [83]. The technique was tested employing 3-D CT information sets from 8
215 healthy individuals. Computer and human analysis showed a 0.8-pixel root mean square
216 difference. A pixel-value threshold was based on slices, together with 02 sets of categorization
217 criteria that incorporate size, circularity, and position data were used to completely automate lung
218 segmentation [84]. They achieved 94.0% segmentation precision with 2969 thick slice images and
219 97.6% with 1161 thin slice images based on 101 CT cases [85]. The lung volume was segmented
220 and visualized using anisotropic filtering and wavelet transform-based interpolation. The
221 robustness and application of the approach were demonstrated using single-detector CT scans,
222 which showed improvements in volume overlap and volume difference percentages.
223 Swierczynski and his team devised a level-set-based segmentation approach that combined
224 traditional segmentation with active dense displaced field prediction [86]. The developed approach
225 performed better than registration and segmentation independent. A substitutional level set
226 technique for CT scan lung nodule segmentation was developed using a global lung nodule form

227 model. [87]. Nodule kind or position did not affect the proposed technique. Moreover, to improve
228 lung nodule detection, a parameter-free segmentation method was developed that focused on
229 juxtapleural lesions [88]. LIDC's 403 juxtapleural nodules indicated a 92.6% re-inclusion rate.
230 Zhang et al. [89] developed an automated lung segmentation approach and a global optimum
231 hybrid geometric active contour model. Incorporating global region and edge information
232 increased algorithm performance in places with narrow bands or weak boundaries. Furthermore,
233 in another study, [90], a sphere was placed within the segmented lung target and deformed in
234 response to forces applied to the lung boundaries. The system was tested on 40 CT images,
235 achieving an average F-measure of 99.22%.

236

237 Researchers have been examining CNNs' durability in computer vision for ten years. Multiple
238 CNN-based methods have been reported for medical and natural image processing. Several
239 methods have been proposed using AI and CT images for the detection of lung cancer [91]. Lung
240 nodule classification was carried out using a three-dimensional CNN with three modules. This
241 technique outperformed manual evaluation with 84.4% sensitivity. Nasser and Naser [92] used an
242 ANN to diagnose lung cancer with 96.67% accuracy. Cifci et al. [93] reported that DL, combined
243 with Instantaneously Trained Neural Networks (DITNN) and Increased Profuse Clustering
244 (IPCT), improved lung image quality and lung cancer detection, achieving an accuracy of 98.42%.
245 Moreover, in another study [94], a double convolutional deep neural network (CDNN) and a
246 regular CDNN were employed to identify lung nodules, achieving an accuracy of 0.909 and 0.872.
247 Wang et al. [95] developed a CAD system with low false negative and positive rates as well as
248 high nodule detection precision. In another approach [96], the deep model achieved 95.41%
249 sensitivity in lung image detection using inception-v3 transfer learning instead of randomized

250 initialization. Finally, a multi-group patch-based learning system was reported, revealing an
251 80.06% sensitivity with 4.7 false positives per scan or a 94% sensitivity with 15.1 false positives
252 per scan. Further, a dense convolutional binary-tree network (DenseBTNet) was developed which
253 showed high parameter effectiveness and extracted features at several scales [97]. Li et al. found
254 that early detection reduces the death rate from lung cancer [98]. They developed a DL-CAD
255 system that could recognize and classify lung nodules under 3 mm and estimate their malignancy
256 risk. The system demonstrated an accuracy of 86.2% in sensitivity testing carried out on the LIDC-
257 IDRI and NLST datasets.
258 Similarly, a deep 3D residual CNN was employed to decrease false positives for automated lung
259 nodule diagnosis in CT images [99]. A spatial pooling and cropping (SPC) layer gathered multi-
260 level contextual information, and their 27-layer network achieved 98.3% sensitivity using the
261 LUNA-16 dataset. Teramoto et al. [100] developed a DCNN comprising convolutional,
262 completely linked, and pooling layers to automatically classify lung cancer. DCNN training
263 employed 76 cancer cases and achieved 71% classification accuracy. In a study, a 3D
264 convolutional neural network was employed for volumetric CT-based computer-aided lung nodule
265 identification [101]. They used the LUNA16 dataset to test their model, which had 3D
266 convolutional, max-pooling, completely linked, and softmax layers. Their findings suggested that
267 3D CNNs significantly improved detection accuracy, achieving a sensitivity of 94.4%.
268 Similarly, DL algorithms were employed to predict lung cancer survival, determine EGFR
269 mutation status, and classify subtypes based on CT scans [102, 103]. Several studies have explored
270 the use of DL algorithms for CT imaging pulmonary nodule segmentation and categorization [35].
271 A 3-D deep-learning model and low-dose chest CT images were employed to develop an end-to-
272 end lung tumor detection system [104]. Shao et al. [105] employed DL algorithms to screen mobile

273 low-dose CT images for lung tumors in resource-constrained areas. Moreover, a model [106] was
274 designed that identified the EGFR mutations and expression of PD-L1 status in non-small-cell
275 lung tumors using CT images. A study [107] provided an in-depth analysis of different DL
276 approaches for identifying and diagnosing lung nodules in CT scans.

277 Deep neural networks were employed to segment lung CT images [11] in addition to
278 categorization. Lakshmanaprabu et al. [108] determined that the DL model achieved the highest
279 classification accuracy of 96.3% for lung tumors using CT data. The application of DL models in
280 chest radiography and lung tumor identification using CT images was investigated by Lee et al.
281 [109], who observed that these models may increase clinical efficacy and accuracy. To identify
282 lung cancer, Bhatia et al., [110] proposed a DL technique with 93.55% sensitivity and 91.5%
283 specificity. Moreover, another model [111] was designed using DL on CT scans to detect
284 expression of PD-L1 in non-small cell lung tumors and predict immune checkpoint suppressor
285 responses for a smaller nodule. Hu and his colleague [112] proposed a DL system for lung cancer
286 stage extraction from CT data with an F1 score of 0.848. A machine learning strategy that can
287 detect preinvasive, benign, and invasive lung nodules on 1-mm-thick CT scans was proposed [74,
288 113] to demonstrate the efficacy of a DL-enhanced CAD system in recognizing them. Deep
289 learning was also used to predict lung cancer with an accuracy of 87.63% [114].

290 Vani and his coworkers [115] developed six DL models (CNN GD, CNN, Inception V3, VGG-16,
291 Resnet-50, and VGG-19) that efficiently identified lung tumors by employing CT scans and
292 histopathology images. CNN-GD outperforms other models in precision, F-score, sensitivity,
293 accuracy, and specificity, achieving 97.86%, 96.39%, 96.79%, and 97.40%, respectively. Shalini
294 et al. [116] presented a 3D-CNN and RNN approach that achieved 95% accuracy in classifying
295 malignant lung nodules. Efficiency can be improved using big-data analytics and cascade

296 classifiers. Abunajm et al. [117] proposed a CNN-based model for primary lung cancer prediction
297 and recognition using CT scan imaging, distinguishing malignant, benign, and normal cases. Initial
298 lung cancer detection improves survival and timing of therapy. The model reduced false positives
299 and achieved an accuracy of 99.45%.
300 In a study [118], radiomics and deep learning were employed for lung cancer identification and
301 treatment. Experts explain that radiomics enables the quantification of medical images, enhancing
302 cancer diagnosis and prognosis. Deep learning systems can be used for data analysis. Deep
303 learning was used to forecast the risk of cardiovascular disorders from low-dose CT scans used to
304 test for lung tumors [119]. The researchers used a massive cardiovascular risk dataset to train a
305 DL system to predict heart disease risk from lung CT images. Moreover, in a study [120], dense
306 clustering and DL were combined to immediately train neural networks to improve lung tumor
307 detection from CT images. They demonstrated the efficiency of their lung nodule detection
308 approach by comparing it with existing lung cancer detection methods. A newly developed DCNN
309 was assessed on a large dataset of CT scans to detect and classify lung nodules in 3D CT images
310 [121]. Zhao et al. [122] proposed a weighted discriminatory extreme learning machine for
311 electronic nasal system lung tumor detection. They were able to differentiate between the two
312 groups by using an electronic nasal device to examine breath samples from lung tumor patients
313 and healthy controls. Chen et al. [123] developed a multimodality attention-guided 3D detection
314 system for non-small cell lung cancer using 18 F-FDG PET/CT images. The accuracy of PET/CT
315 lung cancer detection was improved by the researchers using deep learning algorithms, which
316 could help in early diagnosis and treatment. **Table 1 lists the uses, advantages, and drawbacks of
317 lung imaging technologies, whereas Table 2 lists the studied models from 2018–2022.**

318 **Table 1. Uses, Advantages, and Drawbacks of Lung Imaging Technologies.**

Technology	Uses	Advantages	Drawbacks
CT Imaging	Primary detection of lung tumors; segmentation of lung nodules.	High-resolution imaging; clear separation of lung vs. non-lung areas due to attenuation differences.	Susceptible to heterogeneity, poor contrast variations, noise, and difficulty distinguishing benign from malignant nodules.
MRI Imaging	Delineation of organ/lesion boundaries; morphological assessment.	Improved soft tissue contrast.	Lower spatial resolution for lung structures; higher sensitivity to motion artifacts; less commonly used for lung nodule detection.
EBUS (Endobronchial Ultrasound)	Visualization of internal lung structures; assisting in tumor characterization.	Minimally invasive; provides real-time imaging.	Limited research on CNN interpretation; challenges in differentiating benign from malignant lesions.
Traditional CADx Systems	Automated analysis using hand-crafted features.	Established methodology; less computationally intensive.	Lower accuracy compared to DL-based methods; reliance on manually engineered features that are less robust and adaptable.

320

321

322 **Table 2.** Studied Models for Lung Image Segmentation and Nodule Detection (2018–2022).

Model / Study	Architecture / Method	Key Features / Performance
Basic CNN Model for Lung Segmentation	Single convolution layer (6 kernels), max pooling, 2 fully connected layers; clustering-based training dataset.	Utilizes k-means clustering for dataset creation; evaluated via eightfold cross-validation.
Automated Lung Segmentation via Image Decomposition & Filtering	Combination of image decomposition-based filtering, wavelet transformation, and morphological methods with contour correction.	Denoises CT images while preserving lung outlines.
Residual U-Net for Lung CT Segmentation	Residual U-Net incorporating residual units.	Designed to reduce false positives and extract robust segmentation features.
U-Net vs. E-Net Comparison for Pulmonary Fibrosis Segmentation	Comparative study between U-Net and E-Net architectures.	Achieves fast and effective segmentation of pulmonary fibrosis parenchyma.
U-Net-Based Lung Segmentation with Dual Paths	U-Net variant featuring an expanding path for high-level and contracting path for low-level information.	High segmentation accuracy with a Dice coefficient of 0.9502.
Mask R-CNN-Based Lung Segmentation	Mask R-CNN integrated with supervised and unsupervised machine learning.	Rapid segmentation (11.2 s) with high precision (97.68%).
Multi-View Convolutional Network for Nodule Recognition	Integration of several 2D ConvNet streams with a reliable classification algorithm.	Targets solid, subsolid, and large nodules; 85.4% detection sensitivity with 4 false positives per scan.
3D CNN and FCN for Autonomous Nodule Identification	3D CNN combined with a fully convolutional network (FCN).	Rapid generation of volume score maps; autonomous detection of candidate regions.
Deep Learning with Shape-Driven Level Sets	Combination of deep learning and level set methods for segmentation.	Automatic fine segmentation is initialized by seed points from coarse segmentation.

323

324

325

326 **Developing Techniques for Detecting Lung Cancer**

Preprint

327 Lung cancer is one type of fatal cancer. Identifying cases is challenging because they typically
328 manifest in the terminal stage. However, mortality can be decreased by early disease detection and
329 treatment. CT imaging is a reliable diagnostic method since it can detect all predicted and
330 unexpected lung tumor nodules [124]. However, medical practitioners and radiologists can
331 misunderstand CT scan intensity and anatomical structure, making malignant cell identification
332 difficult [125]. Therefore, computer-aided diagnostic methods are being employed by radiologists
333 and physicians to diagnose cancer [126]. Numerous technologies have been established, and
334 research into lung cancer detection is still ongoing. Certain systems need to be improved to achieve
335 100% detection accuracy.

336 Lung cancer may be cured with the correct medications, early detection, and a precise etiology.
337 Early lung tumor detection is therefore essential, especially when screening high-risk populations
338 such as oil field workers, smokers, fume exposer, and others, for whom new biomarkers are
339 required. The precision of the diagnosis also affects the best course of treatment for lung cancer.
340 Therefore, finding sensitive and precise biomarkers is essential for primary diagnosis. Low-dose
341 CT is used in recent lung cancer screening methods. Compared to cases without screening,
342 NELSON [127] reported that this screening method provides 85% sensitivity and 99% specificity.
343 A recent study [128] demonstrated a false-positive rate of less than 81%, necessitating further
344 imaging or testing due to the high incidence.

345 To explain the lung cancer stage and screening schedule, a brief overview is given here. SCLC and
346 NSCLC are the primary lung cancer subtypes. SCLCs are central tumors that form airway
347 submucosal perihilar masses. Histological studies show that basal bronchial epithelial
348 neuroendocrine cells cause this malignancy. Most cells in this scenario are spindle-shaped,
349 rounded, or small with minimal granular chromatin, cytoplasm, and necrosis [129]. Unlike pure

350 and mixed NSCLC, which may include liver, brain, and bone metastases [130], SCLC has limited
351 or extensive phases [131].

352 This malignancy [132] may be characterized by metastases to the brain, liver, and bones, with its
353 stages classified as either confined or extensive [133]. Limited SCLC includes the ipsilateral
354 mediastinum, mediastinal, or supraclavicular lymph nodes at a single radiation site. It is a
355 supraclavicular lymph node if it is located on the same side as the cancerous chest. However, broad
356 SCLC can extend to the 2nd lung lobe, bone marrow, and lymph nodes. Chest radiography produces
357 more detailed images than a chest CT scan, but it is less sensitive. With these characteristics, a
358 computer-aided diagnostic (CAD) model for chest radiographs would improve detection
359 sensitivity while preserving low false-positive (FP) rates [134].

360 Cytological analysis of sputum, especially many samples, may help diagnose lung cancer and find
361 a core tumor in the larger bronchi. Sputum samples seldom included tiny adenocarcinomas under
362 2 cm that originate from airway ramifications like tiny bronchi, bronchioles, and alveoli [135]. As
363 cigarette exposure has increased and decreased squamous cell carcinomas and adenocarcinomas,
364 this information has become more and more crucial. Several screening investigations found that
365 sputum cytology had a 20–30% sensitivity for primary lung tumors. Early studies found that the
366 quantity and form of cells in deeper airways can alter pre-malignant detection [136]. It was
367 reported [137] that, regular sputum cytology is neither sensitive nor precise for lung cancer
368 screening. White light bronchoscopy is the most common histological lung cancer diagnosis
369 procedure. Bronchoscopy can detect pre-malignant lesions. Tissue biopsies are the recognized
370 method for detecting cancer in general hospitals. The size of lung tissue biopsy specimens is
371 necessary for the histopathological detection of lung cancer subtypes. The first biopsy needs to
372 confirm the diagnosis to avoid recurrent operations that can cause difficulties and delay therapy.

373 Fiber optic bronchoscopy, image-guided trans-thoracic needle aspiration, endobronchial
374 ultrasound, pleural fluid examination (thoracentesis), mediastinoscopy, thoracoscopy, and
375 operation are employed to diagnose lung tumors. These methods are expensive, error-prone, and
376 need numerous samples [138].

377 Spiral CT images enhance peripherally small tumor diagnosis. However, these images show
378 significantly reduced sensitivity for central tumor identification (primarily squamous cell
379 carcinoma) than peripheral tumors [139]. In the National Lung Screening Trial (NLST) using
380 LDCT, 96% of positive screenings were false positives, with over 40% of participants,
381 experiencing at least one positive result [66]. The high frequency of false positive screening results
382 in expensive and intrusive therapies for smokers without malignancies. For diagnosis, screening
383 for lung cancer with low-cost, non-invasive methods is essential.

384 CNN, a kind of DL, has advanced radiology [140, 141]. In chest radiography, DL-based models
385 have also demonstrated success in detecting masses and nodules, with mFPIs of 0.02–0.34 and
386 sensitivities of 0.51–0.84. Moreover, radiologists were able to identify nodules more accurately
387 with CAD models than with screening procedures without them. It might be difficult for
388 radiologists to identify and differentiate between benign and malignant nodules [142, 143].
389 Radiologists also need to monitor nodule form and marginal features as typical anatomical
390 structures mimic healthy nodules. Even the most skilled radiologists may make diagnostic
391 mistakes due to circumstances rather than radiologists [144, 145]. The main DL methods for lesion
392 identification are segmentation and detection. The detection approach labels an area, unlike the
393 segmentation method, which labels pixels. Segmentation provides more exact pixel labels than
394 detection. Pixel-level lesion size categorization enhances clinical diagnosis. Lesion size and form
395 variations are easier to monitor using pixel-level classification because the shape may affect

396 detection. As part of the evaluation of management effectiveness, it also displays lesion size and
397 long and short diameters [146].

398 **Investigation Gaps and Limitations**

399 Better survival rates depend on the primary detection of lung tumors, however, this is difficult
400 because of factors such as heterogeneity, low contrast fluctuations, and visual similarities between
401 benign and malignant nodules in CT images [147]. Identifying lung nodules with medical imaging
402 is challenging owing to the complex architecture and time-consuming acquisition of labeled
403 samples [148]. Deep learning algorithms are frequently compared to traditional CADx systems
404 that employ manually created features, even though they can automatically identify features in
405 lung nodule CT scans [149]. There is limited research on employing CNNs to analyze EBUS
406 images, which makes it challenging to distinguish benign from potentially malignant tumors [150].
407 While some studies have employed CT scans to predict mortality risks in NSCLC patients, they
408 have not identified primary-stage lung or lobe-related malignancies [151]. The mechanism by
409 which CNNs predict nodule malignancy and the influence of area or contextual information on
410 their output remains unclear [152]. Computer-assisted lung disease detection is crucial owing to
411 noise signals affecting cancer image quality during acquisition [153]. Training DCNNs is
412 challenging because of the various kinds of lung nodules and few positive samples inaccessible
413 datasets [154].

414 **Process of Segmentation**

415 Image segmentation shows organ or structural outlines. DL techniques improve semantic
416 segmentation, which makes them useful for medical diagnosis. This method evaluates the sizes
417 and shapes of organs or lesions using MRI or CT scans [155, 156]. Many researchers have
418 proposed automated segmentation methods. However, pre-processing typically involves edge

419 detection and the application of mathematical filters. Further, deep machine learning extracted
420 complex traits. Creating and extracting hand-crafted features was the biggest challenge for such a
421 system, limiting deployment. Medical researchers segmented images using 2D, 2.5D, and 3D CNN
422 [157, 158].

423 A CT scan can easily separate the lung and non-lung areas in a typical lung due to their different
424 image attenuation. Early lung segmentation approaches encompassed numerical methods, gray-
425 level thresholding, and shape-based approaches to distinguish lung regions from non-lung areas.

426 Various CNN-based methods have been established for both medical and natural image
427 processing. Early research focused on lung nodule segmentation [156]. In a study [159], a basic
428 CNN model for lung segmentation was developed employing a clustering algorithm-based training
429 dataset. The k-means clustering technique divided CT slices into two groups using the image
430 patch's mean and minimum intensity. Cross-shaped confirmation, volume intersection, linked
431 component analysis, and patch expansion were used to construct the dataset. The CNN design
432 comprised a single layer of convolution with 6 kernels, one maximally pooled layer, and 02 fully
433 connected layers. An eightfold cross-validation method was employed to evaluate CNN models
434 trained on the produced datasets. The researchers designed automated lung segmentation
435 techniques to denoise lung CT images without affecting lung outlines using an image
436 decomposition-based filtering technique [160]. The lungs were segmented using wavelet
437 transformation and morphological methods. Finally, contour correction was used to smooth the
438 lung outlines during segmentation refinement.

439 Khanna et al. [161] developed a false-positive-reducing Residual U-Net for lung CT segmentation.
440 The more complex network with residual units in the suggested model makes it easier to extract
441 lung segmentation information. However, the performance of U-Net and E-Net was compared

442 [162]. These models partition pulmonary fibrosis parenchyma quickly and effectively.
443 Furthermore, a U-net-based lung segmentation approach was developed that had an expanding
444 route for high-level information and a contracting route for low-level information [163]. The dice
445 coefficient performance was 0.9502 in experiments. Mask R-CNN and supervised and
446 unsupervised machine learning were used to produce another automated lung segmentation
447 method [164]. The benchmarked methods were slower and less precise than our approach, which
448 achieved a segmentation precision of 97.68% and was completed in 11.2 s.
449 Setio et al. presented a multi-view convolution network to recognize lung nodules using training
450 data's discriminative features [165]. The three-nodule potential detectors target solid, subsolid, and
451 large nodules. The proposed method integrates several 2-D ConvNet streams with a reliable
452 classification algorithm. The LIDC-IDRI dataset shows four false positives per scan and 85.4%
453 detection sensitivity. Similarly, a 3D CNN was trained using LIDC dataset volumes of interest to
454 autonomously identify lung nodules [166]. Furthermore, a 3D CNN was employed to quickly
455 produce the volume score map in a single run by generating a 3D fully convolutional network
456 (FCN). Candidate regions of interest were quickly generated by the discriminating CNN using the
457 FCN-based architecture.

458 In another study [167], DL and shape-driven level sets were employed to produce another
459 automatic lung nodule segmentation system. The invention of shape-driven level sets was the first
460 step toward fine segmentation. Similarly, the model was automatically initialized by the level sets
461 using seed points from the deep network's coarse segmentation.

462 **Conclusion and recommendation**

463 This study highlights the significant progress made in pulmonary nodule diagnosis and
464 segmentation through deep learning (DL) techniques. The study addresses issues including

465 heterogeneity, low contrast variations, and the visual similarities between benign and malignant
466 formations in CT imaging by utilizing convolutional neural networks (CNNs) and transfers
467 learning techniques to improve the accuracy of lung nodule identification and delineation. The
468 integration of DL approaches has shown superiority over traditional computer-aided diagnosis
469 (CAD) systems that rely on hand-crafted features, offering a more robust and automated solution
470 for early lung cancer detection.

471 For future research, a deeper exploration of DL model interpretability is crucial to clarify the
472 specific features and contextual information these networks use to distinguish between benign and
473 malignant nodules. Further, expanding the diversity and size of annotated datasets will enhance
474 the generalizability and performance of DL models. Collaborative efforts between
475 multidisciplinary teams, including radiologists, data scientists, and clinicians, are essential to
476 translate these technological advancements into clinical practice, ultimately improving patient
477 outcomes through early and accurate lung cancer diagnosis.

478 **Declarations**

479 **Funding**

480 None

481 **Conflicts of interest**

482 None

483 **Availability of data and material**

484 There are no data associated with this review paper.

485 **Code availability**

486 Not applicable

487 **Ethics approval**

488 **Not applicable**

489 **Consent to participate**

490 Not applicable

491 **Consent for publication**

492 None

493 **Acknowledgment**

494 **None**

495 **Author contribution statement**

496 All authors contributed to the work fulfilling the criteria adopted from ICMJE. Acquisition of data:
497 **YX, YL, FW, YZ and DH**. Analysis and interpretation of data: **YX, YL, FW, YZ, and DH**.
498 Drafting of the manuscript: **YX, YL, FW, YZ, and DH**. Critical revision: **YX, YL, FW, YZ and**
499 **DH**. Study conception and design: WX and WZ. Financial support: WX and WZ. All authors read
500 and approved the submitted version of the manuscript. Each author has agreed both be personally
501 accountable for the author's contributions and to ensure that questions related to the accuracy or
502 integrity of any part of the work, even those in which the author was not personally involved, are
503 appropriately investigated and resolved and that the resolution is documented in the literature.

504

505

506

507

508

509 **References**

- 510 1. Gałązka, J.K., et al., *Obesity and lung cancer – is programmed death ligand-1 (PD-1L) expression*
511 *a connection?* Archives of Medical Science, 2024. **20**(1): p. 313-316.
- 512 2. Thandra, K.C., et al., *Epidemiology of lung cancer*. Contemp Oncol (Pozn), 2021. **25**(1): p. 45-52.
- 513 3. Siegel, R.L., et al., *Cancer Statistics, 2021*. CA Cancer J Clin, 2021. **71**(1): p. 7-33.
- 514 4. Gould, M.K., et al., *Evaluation of individuals with pulmonary nodules: when is it lung cancer?*
515 *Diagnosis and management of lung cancer, 3rd ed: American College of Chest Physicians evidence-*
516 *based clinical practice guidelines*. Chest, 2013. **143**(5 Suppl): p. e93S-e120S.
- 517 5. Bankier, A.A., et al., *Recommendations for Measuring Pulmonary Nodules at CT: A Statement from*
518 *the Fleischner Society*. Radiology, 2017. **285**(2): p. 584-600.
- 519 6. Hansell, D.M., et al., *Fleischner Society: glossary of terms for thoracic imaging*. Radiology, 2008.
520 **246**(3): p. 697-722.
- 521 7. Lu, M.-S., et al., *Appraisal of lung cancer survival in patients with end-stage renal disease*. Archives
522 of Medical Science, 2023. **19**(1): p. 86-93.
- 523 8. Choi, W.J. and T.S. Choi, *Automated pulmonary nodule detection based on three-dimensional*
524 *shape-based feature descriptor*. Comput Methods Programs Biomed, 2014. **113**(1): p. 37-54.
- 525 9. Peloschek, P., et al., *Pulmonary nodules: sensitivity of maximum intensity projection versus that of*
526 *volume rendering of 3D multidetector CT data*. Radiology, 2007. **243**(2): p. 561-9.
- 527 10. Kim, H., et al., *Pulmonary subsolid nodules: what radiologists need to know about the imaging*
528 *features and management strategy*. Diagn Interv Radiol, 2014. **20**(1): p. 47-57.
- 529 11. Revel, M.-P., et al., *Are two-dimensional CT measurements of small noncalcified pulmonary*
530 *nodules reliable?* Radiology, 2004. **231**(2): p. 453-458.
- 531 12. Han, D., M.A. Heuvelmans, and M. Oudkerk, *Volume versus diameter assessment of small*
532 *pulmonary nodules in CT lung cancer screening*. Translational lung cancer research, 2017. **6**(1): p.
533 52.
- 534 13. Brzozowska, M., et al., *Overall survival of patients with EGFR mutation-positive non-small-cell lung*
535 *cancer treated with erlotinib, gefitinib or afatinib under drug programmes in Poland – real-world*
536 *data*. Archives of Medical Science, 2021. **17**(6): p. 1618-1627.
- 537 14. Henschke, C.I., et al., *Early Lung Cancer Action Project: overall design and findings from baseline*
538 *screening*. The Lancet, 1999. **354**(9173): p. 99-105.
- 539 15. Castellino, R.A., *Computer aided detection (CAD): an overview*. Cancer Imaging, 2005. **5**(1): p. 17.
- 540 16. McCarville, M.B., et al., *Distinguishing benign from malignant pulmonary nodules with helical*
541 *chest CT in children with malignant solid tumors*. Radiology, 2006. **239**(2): p. 514-520.
- 542 17. Singh, S., et al., *Computer-aided classification of breast masses: performance and interobserver*
543 *variability of expert radiologists versus residents*. Radiology, 2011. **258**(1): p. 73-80.
- 544 18. Giger, M.L., N. Karssemeijer, and J.A. Schnabel, *Breast image analysis for risk assessment,*
545 *detection, diagnosis, and treatment of cancer*. Annu Rev Biomed Eng, 2013. **15**: p. 327-57.
- 546 19. Joo, S., et al., *Computer-aided diagnosis of solid breast nodules: use of an artificial neural network*
547 *based on multiple sonographic features*. IEEE transactions on medical imaging, 2004. **23**(10): p.
548 1292-1300.
- 549 20. Way, T.W., et al., *Computer-aided diagnosis of pulmonary nodules on CT scans: improvement of*
550 *classification performance with nodule surface features*. Medical physics, 2009. **36**(7): p. 3086-
551 3098.
- 552 21. Way, T.W., et al., *Computer-aided diagnosis of pulmonary nodules on CT scans: segmentation and*
553 *classification using 3D active contours*. Med Phys, 2006. **33**(7): p. 2323-37.

- 554 22. Giger, M.L., et al., *Computerized detection of pulmonary nodules in digital chest images: Use of*
555 *morphological filters in reducing false-positive detections*. Medical Physics, 1990. **17**(5): p. 861-
556 865.
- 557 23. Ying, W., et al. *Segmentation of regions of interest in lung CT images based on 2-D OTSU optimized*
558 *by genetic algorithm*. in *2009 Chinese Control and Decision Conference*. 2009. IEEE.
- 559 24. Helen, R., et al. *Segmentation of pulmonary parenchyma in CT lung images based on 2D Otsu*
560 *optimized by PSO*. in *2011 international conference on emerging trends in electrical and computer*
561 *technology*. 2011. IEEE.
- 562 25. Liu, Y., et al. *Hidden conditional random field for lung nodule detection*. in *2014 IEEE International*
563 *Conference on Image Processing (ICIP)*. 2014. IEEE.
- 564 26. John, J. and M. Mini, *Multilevel thresholding based segmentation and feature extraction for*
565 *pulmonary nodule detection*. Procedia Technology, 2016. **24**: p. 957-963.
- 566 27. Teramoto, A., et al., *Automated detection of pulmonary nodules in PET/CT images: Ensemble false-*
567 *positive reduction using a convolutional neural network technique*. Med Phys, 2016. **43**(6): p. 2821-
568 2827.
- 569 28. Mastouri, R., et al. *A morphological operation-based approach for Sub-pleural lung nodule*
570 *detection from CT images*. in *2018 IEEE 4th Middle East Conference on Biomedical Engineering*
571 *(MECBME)*. 2018. IEEE.
- 572 29. Santos, A.M., et al., *Automatic detection of small lung nodules in 3D CT data using Gaussian*
573 *mixture models, Tsallis entropy and SVM*. Engineering applications of artificial intelligence, 2014.
574 **36**: p. 27-39.
- 575 30. Alfaro, M.d.J.N., et al., *Automated system for lung nodules classification based on wavelet feature*
576 *descriptor and support vector machine*. 2015.
- 577 31. Lu, L., et al., *Hybrid detection of lung nodules on CT scan images*. Med Phys, 2015. **42**(9): p. 5042-
578 54.
- 579 32. Farahani, F.V., A. Ahmadi, and M.F. Zarandi. *Lung nodule diagnosis from CT images based on*
580 *ensemble learning*. in *2015 IEEE Conference on Computational Intelligence in Bioinformatics and*
581 *Computational Biology (CIBCB)*. 2015. IEEE.
- 582 33. Klik, M., et al. *Improved classification of pulmonary nodules by automated detection of benign*
583 *subpleural lymph nodes*. in *3rd IEEE International Symposium on Biomedical Imaging: Nano to*
584 *Macro, 2006*. 2006. IEEE.
- 585 34. Froz, B.R., et al., *Lung nodule classification using artificial crawlers, directional texture and support*
586 *vector machine*. Expert Systems with Applications, 2017. **69**: p. 176-188.
- 587 35. Wu, J. and T. Qian, *A survey of pulmonary nodule detection, segmentation and classification in*
588 *computed tomography with deep learning techniques*. Journal of Medical Artificial Intelligence,
589 2019. **2**.
- 590 36. Liu, K., et al., *Evaluating a fully automated pulmonary nodule detection approach and its impact*
591 *on radiologist performance*. Radiology: Artificial Intelligence, 2019. **1**(3): p. e180084.
- 592 37. Shen, W., et al. *Multi-scale convolutional neural networks for lung nodule classification*. in
593 *Information Processing in Medical Imaging: 24th International Conference, IPMI 2015, Sabhal Mor*
594 *Ostaig, Isle of Skye, UK, June 28-July 3, 2015, Proceedings 24*. 2015. Springer.
- 595 38. Ciompi, F., et al., *Towards automatic pulmonary nodule management in lung cancer screening with*
596 *deep learning*. Sci Rep, 2017. **7**: p. 46479.
- 597 39. Causey, J.L., et al., *Highly accurate model for prediction of lung nodule malignancy with CT scans*.
598 Scientific reports, 2018. **8**(1): p. 9286.
- 599 40. Hua, K.-L., et al., *Computer-aided classification of lung nodules on computed tomography images*
600 *via deep learning technique*. OncoTargets and therapy, 2015: p. 2015-2022.

- 601 41. Hensley, C.P. and A.J. Emerson, *Non-Small Cell Lung Carcinoma: Clinical Reasoning in the*
602 *Management of a Patient Referred to Physical Therapy for Costochondritis*. *Physical Therapy*, 2018.
603 **98**(6): p. 503-509.
- 604 42. Dhara, A.K., S. Mukhopadhyay, and N. Khandelwal, *Computer-aided detection and analysis of*
605 *pulmonary nodule from CT images: a survey*. *IETE Technical Review*, 2012. **29**(4): p. 265-275.
- 606 43. Sluimer, I., et al., *Computer analysis of computed tomography scans of the lung: a survey*. *IEEE*
607 *Trans Med Imaging*, 2006. **25**(4): p. 385-405.
- 608 44. Valente, I.R.S., et al., *Automatic 3D pulmonary nodule detection in CT images: a survey*. *Computer*
609 *methods and programs in biomedicine*, 2016. **124**: p. 91-107.
- 610 45. Halder, A., D. Dey, and A.K. Sadhu, *Lung Nodule Detection from Feature Engineering to Deep*
611 *Learning in Thoracic CT Images: a Comprehensive Review*. *J Digit Imaging*, 2020. **33**(3): p. 655-677.
- 612 46. Zhang, G., et al., *Automatic nodule detection for lung cancer in CT images: A review*. *Computers in*
613 *biology and medicine*, 2018. **103**: p. 287-300.
- 614 47. Gu, Y., et al., *A survey of computer-aided diagnosis of lung nodules from CT scans using deep*
615 *learning*. *Comput Biol Med*, 2021. **137**: p. 104806.
- 616 48. Monkam, P., et al., *Detection and classification of pulmonary nodules using convolutional neural*
617 *networks: a survey*. *IEEE Access*, 2019. **7**: p. 78075-78091.
- 618 49. Rubin, G.D., *Lung nodule and cancer detection in computed tomography screening*. *J Thorac*
619 *Imaging*, 2015. **30**(2): p. 130-8.
- 620 50. Scholten, E.T., et al., *Computed tomographic characteristics of interval and post screen carcinomas*
621 *in lung cancer screening*. *European radiology*, 2015. **25**: p. 81-88.
- 622 51. Nair, A., et al., *The impact of trained radiographers as concurrent readers on performance and*
623 *reading time of experienced radiologists in the UK Lung Cancer Screening (UKLS) trial*. *European*
624 *Radiology*, 2018. **28**: p. 226-234.
- 625 52. Matsumoto, S., et al., *Computer-aided detection of lung nodules on multidetector CT in concurrent-*
626 *reader and second-reader modes: a comparative study*. *European journal of radiology*, 2013. **82**(8):
627 p. 1332-1337.
- 628 53. Yang, Y., et al., *Deep learning aided decision support for pulmonary nodules diagnosing: a review*.
629 *Journal of thoracic disease*, 2018. **10**(Suppl 7): p. S867.
- 630 54. Horeweg, N., et al., *Detection of lung cancer through low-dose CT screening (NELSON): a*
631 *prespecified analysis of screening test performance and interval cancers*. *The Lancet Oncology*,
632 2014. **15**(12): p. 1342-1350.
- 633 55. Goo, J.M., *A computer-aided diagnosis for evaluating lung nodules on chest CT: the current status*
634 *and perspective*. *Korean J Radiol*, 2011. **12**(2): p. 145-55.
- 635 56. Korst, R.J., et al., *The utility of automated volumetric growth analysis in a dedicated pulmonary*
636 *nodule clinic*. *The Journal of Thoracic and Cardiovascular Surgery*, 2011. **142**(2): p. 372-377.
- 637 57. Ko, J.P., et al., *Pulmonary nodules: growth rate assessment in patients by using serial CT and three-*
638 *dimensional volumetry*. *Radiology*, 2012. **262**(2): p. 662-671.
- 639 58. Kuhnigk, J.M., et al., *Morphological segmentation and partial volume analysis for volumetry of*
640 *solid pulmonary lesions in thoracic CT scans*. *IEEE Trans Med Imaging*, 2006. **25**(4): p. 417-34.
- 641 59. Devaraj, A., et al., *Use of Volumetry for Lung Nodule Management: Theory and Practice*. *Radiology*,
642 2017. **284**(3): p. 630-644.
- 643 60. de Hoop, B., et al., *A comparison of six software packages for evaluation of solid lung nodules*
644 *using semi-automated volumetry: what is the minimum increase in size to detect growth in*
645 *repeated CT examinations*. *Eur Radiol*, 2009. **19**(4): p. 800-8.
- 646 61. Callister, M.E., et al., *British Thoracic Society guidelines for the investigation and management of*
647 *pulmonary nodules*. *Thorax*, 2015. **70 Suppl 2**: p. ii1-ii54.

- 648 62. Kadir, T. and F. Gleeson, *Lung cancer prediction using machine learning and advanced imaging*
649 *techniques*. *Transl Lung Cancer Res*, 2018. **7**(3): p. 304-312.
- 650 63. Sung, H., et al., *Global Cancer Statistics 2020: GLOBOCAN Estimates of Incidence and Mortality*
651 *Worldwide for 36 Cancers in 185 Countries*. *CA Cancer J Clin*, 2021. **71**(3): p. 209-249.
- 652 64. Birring, S.S. and M.D. Peake, *Symptoms and the early diagnosis of lung cancer*. *Thorax*, 2005. **60**(4):
653 p. 268-9.
- 654 65. Cataldo, J.K., *High-risk older smokers' perceptions, attitudes, and beliefs about lung cancer*
655 *screening*. *Cancer Med*, 2016. **5**(4): p. 753-9.
- 656 66. Aberle, D.R., et al., *Reduced lung-cancer mortality with low-dose computed tomographic*
657 *screening*. *N Engl J Med*, 2011. **365**(5): p. 395-409.
- 658 67. de Koning, H.J., et al., *Reduced Lung-Cancer Mortality with Volume CT Screening in a Randomized*
659 *Trial*. *N Engl J Med*, 2020. **382**(6): p. 503-513.
- 660 68. Gould, M.K., et al., *Recent Trends in the Identification of Incidental Pulmonary Nodules*. *Am J Respir*
661 *Crit Care Med*, 2015. **192**(10): p. 1208-14.
- 662 69. Hendrix, W., et al., *Trends in the incidence of pulmonary nodules in chest computed tomography:*
663 *10-year results from two Dutch hospitals*. *Eur Radiol*, 2023. **33**(11): p. 8279-8288.
- 664 70. Bruls, R.J.M. and R.M. Kwee, *Workload for radiologists during on-call hours: dramatic increase in*
665 *the past 15 years*. *Insights Imaging*, 2020. **11**(1): p. 121.
- 666 71. Murchison, J.T., et al., *Validation of a deep learning computer aided system for CT based lung*
667 *nodule detection, classification, and growth rate estimation in a routine clinical population*. *PLoS*
668 *One*, 2022. **17**(5): p. e0266799.
- 669 72. Jacobs, C., et al., *Assisted versus Manual Interpretation of Low-Dose CT Scans for Lung Cancer*
670 *Screening: Impact on Lung-RADS Agreement*. *Radiol Imaging Cancer*, 2021. **3**(5): p. e200160.
- 671 73. Hempel, H.L., et al., *Higher agreement between readers with deep learning CAD software for*
672 *reporting pulmonary nodules on CT*. *Eur J Radiol Open*, 2022. **9**: p. 100435.
- 673 74. Kozuka, T., et al., *Efficiency of a computer-aided diagnosis (CAD) system with deep learning in*
674 *detection of pulmonary nodules on 1-mm-thick images of computed tomography*. *Jpn J Radiol*,
675 2020. **38**(11): p. 1052-1061.
- 676 75. Cellina, M., et al., *Artificial Intelligence in Lung Cancer Screening: The Future Is Now*. *Cancers*
677 (Basel), 2023. **15**(17).
- 678 76. Way, T., et al., *Computer-aided diagnosis of lung nodules on CT scans: ROC study of its effect on*
679 *radiologists' performance*. *Acad Radiol*, 2010. **17**(3): p. 323-32.
- 680 77. Vu, H., et al., *fMRI volume classification using a 3D convolutional neural network robust to shifted*
681 *and scaled neuronal activations*. *NeuroImage*, 2020. **223**: p. 117328.
- 682 78. Celeghin, A., et al., *Convolutional neural networks for vision neuroscience: significance,*
683 *developments, and outstanding issues*. *Frontiers in Computational Neuroscience*, 2023. **17**.
- 684 79. Lundervold, A.S. and A. Lundervold, *An overview of deep learning in medical imaging focusing on*
685 *MRI*. *Zeitschrift für Medizinische Physik*, 2019. **29**(2): p. 102-127.
- 686 80. Thanoon, M.A., et al., *A Review of Deep Learning Techniques for Lung Cancer Screening and*
687 *Diagnosis Based on CT Images*. *Diagnostics (Basel)*, 2023. **13**(16).
- 688 81. Brown, M.S., et al., *Method for segmenting chest CT image data using an anatomical model:*
689 *preliminary results*. *IEEE transactions on medical imaging*, 1997. **16**(6): p. 828-839.
- 690 82. Brown, M.S., et al., *Knowledge-based segmentation of thoracic computed tomography images for*
691 *assessment of split lung function*. *Med Phys*, 2000. **27**(3): p. 592-8.
- 692 83. Hu, S., E.A. Hoffman, and J.M. Reinhardt, *Automatic lung segmentation for accurate quantitation*
693 *of volumetric X-ray CT images*. *IEEE Trans Med Imaging*, 2001. **20**(6): p. 490-8.
- 694 84. Leader, J.K., et al., *Automated lung segmentation in X-ray computed tomography: development*
and *evaluation of a heuristic threshold-based scheme*. *Acad Radiol*, 2003. **10**(11): p. 1224-36.

- 696 85. Sun, X., H. Zhang, and H. Duan, *3D computerized segmentation of lung volume with computed*
697 *tomography*. Acad Radiol, 2006. **13**(6): p. 670-7.
- 698 86. Swierczynski, P., et al., *A level-set approach to joint image segmentation and registration with*
699 *application to CT lung imaging*. Comput Med Imaging Graph, 2018. **65**: p. 58-68.
- 700 87. Farag, A.A., et al., *A novel approach for lung nodules segmentation in chest CT using level sets*.
701 IEEE Trans Image Process, 2013. **22**(12): p. 5202-13.
- 702 88. Shen, S., et al., *An automated lung segmentation approach using bidirectional chain codes to*
703 *improve nodule detection accuracy*. Comput Biol Med, 2015. **57**: p. 139-49.
- 704 89. Zhang, W., et al., *Global optimal hybrid geometric active contour for automated lung segmentation*
705 *on CT images*. Comput Biol Med, 2017. **91**: p. 168-180.
- 706 90. Rebouças Filho, P.P., et al., *Novel and powerful 3D adaptive crisp active contour method applied in*
707 *the segmentation of CT lung images*. Med Image Anal, 2017. **35**: p. 503-516.
- 708 91. Zhang, C., et al., *Toward an Expert Level of Lung Cancer Detection and Classification Using a Deep*
709 *Convolutional Neural Network*. Oncologist, 2019. **24**(9): p. 1159-1165.
- 710 92. Nasser, I.M. and S.S. Abu-Naser, *Lung cancer detection using artificial neural network*.
711 International Journal of Engineering and Information Systems (IJEAIS), 2019. **3**(3): p. 17-23.
- 712 93. Cifci, M.A., *SegChaNet: A Novel Model for Lung Cancer Segmentation in CT Scans*. Appl Bionics
713 Biomech, 2022. **2022**: p. 1139587.
- 714 94. Jakimovski, G. and D. Davcev, *Using double convolution neural network for lung cancer stage*
715 *detection*. Applied Sciences, 2019. **9**(3): p. 427.
- 716 95. Wang, J., et al., *Pulmonary nodule detection in volumetric chest CT scans using CNNs-based*
717 *nodule-size-adaptive detection and classification*. IEEE access, 2019. **7**: p. 46033-46044.
- 718 96. Wang, C., et al., *Pulmonary image classification based on inception-v3 transfer learning model*.
719 IEEE Access, 2019. **7**: p. 146533-146541.
- 720 97. Liu, Y., et al., *Dense convolutional binary-tree networks for lung nodule classification*. IEEE Access,
721 2018. **6**: p. 49080-49088.
- 722 98. Li, L., et al., *Evaluating the performance of a deep learning-based computer-aided diagnosis (DL-*
723 *CAD) system for detecting and characterizing lung nodules: Comparison with the performance of*
724 *double reading by radiologists*. Thorac Cancer, 2019. **10**(2): p. 183-192.
- 725 99. Jin, H., et al., *A deep 3D residual CNN for false-positive reduction in pulmonary nodule detection*.
726 Medical physics, 2018. **45**(5): p. 2097-2107.
- 727 100. Teramoto, A., et al., *Automated Classification of Lung Cancer Types from Cytological Images Using*
728 *Deep Convolutional Neural Networks*. Biomed Res Int, 2017. **2017**: p. 4067832.
- 729 101. Dou, Q., et al., *Multilevel contextual 3-D CNNs for false positive reduction in pulmonary nodule*
730 *detection*. IEEE Transactions on Biomedical Engineering, 2016. **64**(7): p. 1558-1567.
- 731 102. Wang, S., et al., *Predicting EGFR mutation status in lung adenocarcinoma on computed*
732 *tomography image using deep learning*. Eur Respir J, 2019. **53**(3).
- 733 103. Wang, C., et al., *Deep learning for predicting subtype classification and survival of lung*
734 *adenocarcinoma on computed tomography*. Transl Oncol, 2021. **14**(8): p. 101141.
- 735 104. Ardila, D., et al., *End-to-end lung cancer screening with three-dimensional deep learning on low-*
736 *dose chest computed tomography*. Nat Med, 2019. **25**(6): p. 954-961.
- 737 105. Shao, J., et al., *Deep Learning Empowers Lung Cancer Screening Based on Mobile Low-Dose*
738 *Computed Tomography in Resource-Constrained Sites*. Front Biosci (Landmark Ed), 2022. **27**(7): p.
739 212.
- 740 106. Wang, C., et al., *Deep Learning to Predict EGFR Mutation and PD-L1 Expression Status in Non-*
741 *Small-Cell Lung Cancer on Computed Tomography Images*. J Oncol, 2021. **2021**: p. 5499385.
- 742 107. Li, R., et al., *Deep Learning Applications in Computed Tomography Images for Pulmonary Nodule*
743 *Detection and Diagnosis: A Review*. Diagnostics (Basel), 2022. **12**(2).

744 108. Lakshmanaprabu, S., et al., *Optimal deep learning model for classification of lung cancer on CT*
745 *images*. Future Generation Computer Systems, 2019. **92**: p. 374-382.

746 109. Lee, S.M., et al., *Deep Learning Applications in Chest Radiography and Computed Tomography:*
747 *Current State of the Art*. J Thorac Imaging, 2019. **34**(2): p. 75-85.

748 110. Bhatia, S., Y. Sinha, and L. Goel. *Lung cancer detection: a deep learning approach*. in *Soft*
749 *Computing for Problem Solving: SocProS 2017, Volume 2*. 2019. Springer.

750 111. Tian, P., et al., *Assessing PD-L1 expression in non-small cell lung cancer and predicting responses*
751 *to immune checkpoint inhibitors using deep learning on computed tomography images*.
752 *Theranostics*, 2021. **11**(5): p. 2098-2107.

753 112. Hu, D., et al., *Automatic extraction of lung cancer staging information from computed tomography*
754 *reports: deep learning approach*. JMIR medical informatics, 2021. **9**(7): p. e27955.

755 113. Ashraf, S.F., et al., *Predicting benign, preinvasive, and invasive lung nodules on computed*
756 *tomography scans using machine learning*. J Thorac Cardiovasc Surg, 2022. **163**(4): p. 1496-
757 1505.e10.

758 114. Subramanian, R.R., et al., *Lung cancer prediction using deep learning framework*. International
759 *Journal of Control and Automation*, 2020. **13**(3): p. 154-160.

760 115. Rajasekar, V., et al., *Lung cancer disease prediction with CT scan and histopathological images*
761 *feature analysis using deep learning techniques*. Results in Engineering, 2023. **18**: p. 101111.

762 116. Wankhade, S. and S. Vigneshwari, *A novel hybrid deep learning method for early detection of lung*
763 *cancer using neural networks*. Healthcare Analytics, 2023. **3**: p. 100195.

764 117. Abunajm, S., et al., *Deep learning approach for early stage lung cancer detection*. arXiv preprint
765 arXiv:2302.02456, 2023.

766 118. Avanzo, M., et al., *Radiomics and deep learning in lung cancer*. Strahlenther Onkol, 2020. **196**(10):
767 p. 879-887.

768 119. Chao, H., et al., *Deep learning predicts cardiovascular disease risks from lung cancer screening low*
769 *dose computed tomography*. Nat Commun, 2021. **12**(1): p. 2963.

770 120. Shakeel, P.M., M.A. Burhanuddin, and M.I. Desa, *Lung cancer detection from CT image using*
771 *improved profuse clustering and deep learning instantaneously trained neural networks*.
772 *Measurement*, 2019. **145**: p. 702-712.

773 121. Zhang, Q., et al., *Lung nodule diagnosis on 3D computed tomography images using deep*
774 *convolutional neural networks*. Procedia Manufacturing, 2019. **39**: p. 363-370.

775 122. Zhao, L., et al., *A weighted discriminative extreme learning machine design for lung cancer*
776 *detection by an electronic nose system*. IEEE Transactions on Instrumentation and Measurement,
777 2021. **70**: p. 1-9.

778 123. Chen, L., et al., *Multimodality Attention-Guided 3-D Detection of Nonsmall Cell Lung Cancer in 18*
779 *F-FDG PET/CT Images*. IEEE Transactions on Radiation and Plasma Medical Sciences, 2021. **6**(4): p.
780 421-432.

781 124. Gindi, A., T.A. Attiatalla, and M.M. Sami, *A comparative study for comparing two feature extraction*
782 *methods and two classifiers in classification of earlystage lung cancer diagnosis of chest x-ray*
783 *images*. Journal of American Science, 2014. **10**(6): p. 13-22.

784 125. Suzuki, K., et al., *Radiologic classification of small adenocarcinoma of the lung: radiologic-*
785 *pathologic correlation and its prognostic impact*. Ann Thorac Surg, 2006. **81**(2): p. 413-9.

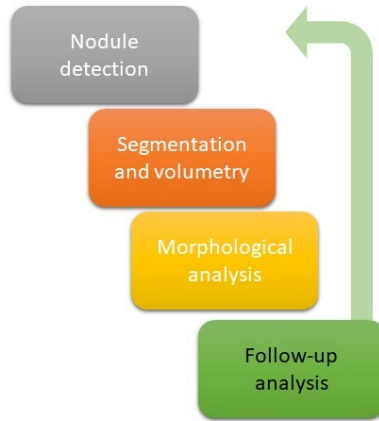
786 126. Wang, H., et al., *Multilevel binomial logistic prediction model for malignant pulmonary nodules*
787 *based on texture features of CT image*. European journal of radiology, 2010. **74**(1): p. 124-129.

788 127. Horeweg, N., et al., *Detection of lung cancer through low-dose CT screening (NELSON): a*
789 *prespecified analysis of screening test performance and interval cancers*. Lancet Oncol, 2014.
790 **15**(12): p. 1342-50.

- 791 128. Gartman, E., et al., *Providence VA lung cancer screening program: performance: comparison of*
792 *local false positive and invasive procedure rates to published trial data*, in *A98. Clinical strategies*
793 *to improve lung cancer early detection: who is at risk here?* 2018, American Thoracic Society. p.
794 A2477-A2477.
- 795 129. Abbas, A.K., N. Fausto, and S.L. Robbins, *Robbins and Cotran pathologic basis of disease*. 2005:
796 Elsevier Saunders.
- 797 130. Travis, W.D., *Update on small cell carcinoma and its differentiation from squamous cell carcinoma*
798 *and other non-small cell carcinomas*. *Modern Pathology*, 2012. **25**: p. S18-S30.
- 799 131. Chan, B.A. and J.I. Coward, *Chemotherapy advances in small-cell lung cancer*. *Journal of thoracic*
800 *disease*, 2013. **5**(Suppl 5): p. S565.
- 801 132. Sagawa, M., et al., *The efficacy of lung cancer screening conducted in 1990s: four case-control*
802 *studies in Japan*. *Lung Cancer*, 2003. **41**(1): p. 29-36.
- 803 133. Fontana, R.S., et al., *Lung cancer screening: the Mayo program*. *Journal of Occupational and*
804 *Environmental Medicine*, 1986. **28**(8): p. 746-750.
- 805 134. Kubik, A., et al., *Lack of benefit from semi-annual screening for cancer of the lung: follow-up report*
806 *of a randomized controlled trial on a population of high-risk males in Czechoslovakia*. *International*
807 *journal of cancer*, 1990. **45**(1): p. 26-33.
- 808 135. Raghu, V.K., et al., *Feasibility of lung cancer prediction from low-dose CT scan and smoking factors*
809 *using causal models*. *Thorax*, 2019. **74**(7): p. 643-649.
- 810 136. Risse, E.K., G.P. Vooijs, and M.A. van't Hof, *Relationship between the cellular composition of*
811 *sputum and the cytologic diagnosis of lung cancer*. *Acta Cytol*, 1987. **31**(2): p. 170-6.
- 812 137. MacDougall, B. and B. Weirnerman, *The value of sputum cytology*. *Journal of general internal*
813 *medicine*, 1992. **7**: p. 11-13.
- 814 138. Kennedy, T., et al., *A randomized study of fluorescence bronchoscopy versus white-light*
815 *bronchoscopy for early detection of lung cancer in high risk patients*. *Lung Cancer*, 2000. **1**(29): p.
816 244-245.
- 817 139. Toyoda, Y., et al., *Sensitivity and specificity of lung cancer screening using chest low-dose computed*
818 *tomography*. *Br J Cancer*, 2008. **98**(10): p. 1602-7.
- 819 140. Hinton, G., *Deep learning—a technology with the potential to transform health care*. *Jama*, 2018.
820 **320**(11): p. 1101-1102.
- 821 141. LeCun, Y., Y. Bengio, and G. Hinton, *Deep learning*. *nature*, 2015. **521**(7553): p. 436-444.
- 822 142. Ueda, D., A. Shimazaki, and Y. Miki, *Technical and clinical overview of deep learning in radiology*.
823 *Jpn J Radiol*, 2019. **37**(1): p. 15-33.
- 824 143. Nam, J.G., et al., *Development and validation of deep learning–based automatic detection*
825 *algorithm for malignant pulmonary nodules on chest radiographs*. *Radiology*, 2019. **290**(1): p. 218-
826 228.
- 827 144. Manser, R., et al., *Screening for lung cancer*. *Cochrane database of systematic reviews*, 2013(6).
- 828 145. Berlin, L., *Radiologic errors, past, present and future*. *Diagnosis (Berl)*, 2014. **1**(1): p. 79-84.
- 829 146. Schwartz, L.H., et al., *RECIST 1.1-Update and clarification: From the RECIST committee*. *Eur J*
830 *Cancer*, 2016. **62**: p. 132-7.
- 831 147. Schwyzer, M., et al., *Automated detection of lung cancer at ultralow dose PET/CT by deep neural*
832 *networks - Initial results*. *Lung Cancer*, 2018. **126**: p. 170-173.
- 833 148. Sun, W., B. Zheng, and W. Qian, *Automatic feature learning using multichannel ROI based on deep*
834 *structured algorithms for computerized lung cancer diagnosis*. *Computers in biology and medicine*,
835 2017. **89**: p. 530-539.
- 836 149. Hosny, A., et al., *Deep learning for lung cancer prognostication: a retrospective multi-cohort*
837 *radiomics study*. *PLoS medicine*, 2018. **15**(11): p. e1002711.

- 838 150. Tiwari, L., et al., *Detection of lung nodule and cancer using novel Mask-3 FCM and TWEDLNN*
839 *algorithms*. Measurement, 2021. **172**: p. 108882.
- 840 151. Wu, B., et al. *Joint learning for pulmonary nodule segmentation, attributes and malignancy*
841 *prediction*. in *2018 IEEE 15th international symposium on biomedical imaging (ISBI 2018)*. 2018.
842 IEEE.
- 843 152. Liu, H., et al., *Multi-model ensemble learning architecture based on 3D CNN for lung nodule*
844 *malignancy suspiciousness classification*. Journal of Digital Imaging, 2020. **33**: p. 1242-1256.
- 845 153. Li, J., Y. Tao, and T. Cai, *Predicting lung cancers using epidemiological data: A generative-*
846 *discriminative framework*. IEEE/CAA Journal of Automatica Sinica, 2021. **8**(5): p. 1067-1078.
- 847 154. Xie, Y., J. Zhang, and Y. Xia, *Semi-supervised adversarial model for benign–malignant lung nodule*
848 *classification on chest CT*. Medical image analysis, 2019. **57**: p. 237-248.
- 849 155. Abdani, S.R., et al., *Computer-Assisted Pterygium Screening System: A Review*. Diagnostics (Basel),
850 2022. **12**(3).
- 851 156. Zulkifley, M.A., et al., *Automated apple recognition system using semantic segmentation networks*
852 *with group and shuffle operators*. Agriculture, 2022. **12**(6): p. 756.
- 853 157. Stofa, M.M., M.A. Zulkifley, and M.A.A.M. Zainuri, *Skin lesions classification and segmentation: a*
854 *review*. International Journal of Advanced Computer Science and Applications, 2021. **12**(10).
- 855 158. Stofa, M.M., et al. *U-net with atrous spatial pyramid pooling for skin lesion segmentation*. in
856 *Proceedings of the 6th International Conference on Electrical, Control and Computer Engineering:*
857 *InECCE2021, Kuantan, Pahang, Malaysia, 23rd August. 2022*. Springer.
- 858 159. Xu, M., et al., *Segmentation of lung parenchyma in CT images using CNN trained with the clustering*
859 *algorithm generated dataset*. Biomedical engineering online, 2019. **18**: p. 1-21.
- 860 160. Liu, C. and M. Pang, *Automatic lung segmentation based on image decomposition and wavelet*
861 *transform*. Biomedical Signal Processing and Control, 2020. **61**: p. 102032.
- 862 161. Khanna, A., et al., *A deep Residual U-Net convolutional neural network for automated lung*
863 *segmentation in computed tomography images*. Biocybernetics and Biomedical Engineering,
864 2020. **40**(3): p. 1314-1327.
- 865 162. Comelli, A., et al., *Lung segmentation on high-resolution computerized tomography images using*
866 *deep learning: a preliminary step for radiomics studies*. Journal of Imaging, 2020. **6**(11): p. 125.
- 867 163. Skourt, B.A., A. El Hassani, and A. Majda, *Lung CT image segmentation using deep neural networks*.
868 *Procedia Computer Science*, 2018. **127**: p. 109-113.
- 869 164. Hu, Q., et al., *An effective approach for CT lung segmentation using mask region-based*
870 *convolutional neural networks*. Artif Intell Med, 2020. **103**: p. 101792.
- 871 165. Setio, A.A.A., et al., *Pulmonary nodule detection in CT images: false positive reduction using multi-*
872 *view convolutional networks*. IEEE transactions on medical imaging, 2016. **35**(5): p. 1160-1169.
- 873 166. Negahdar, M., D. Beymer, and T. Syeda-Mahmood. *Automated volumetric lung segmentation of*
874 *thoracic CT images using fully convolutional neural network*. in *Medical Imaging 2018: Computer-*
875 *Aided Diagnosis*. 2018. SPIE.
- 876 167. Roy, R., T. Chakraborti, and A.S. Chowdhury, *A deep learning-shape driven level set synergism for*
877 *pulmonary nodule segmentation*. Pattern Recognition Letters, 2019. **123**: p. 31-38.

878



Preprint